ELSEVIER

LIVER

Noninvasive Positive Pressure Ventilation to Prevent Respiratory Collapse after Extubation: Clinical Case Reports

S. Nagai, Y. Fujimoto, H. Kamei, T. Nakamura, and T. Kiuchi

ABSTRACT

Respiratory complications often develop in liver transplant recipients, and appropriate respiratory management is crucial to improve patient outcome. To evaluate the clinical usefulness of noninvasive positive pressure ventilation (NPPV) in liver transplant recipients, we established application criteria for NPPV in respiratory management in these patients, as follows: (1) arterial oxygen tension to fraction of inspired oxygen ratio less than 300 and arterial carbon dioxide tension greater than 45 mm Hg; (2) arterial oxygen tension to fraction of inspired oxygen ratio less than 200; (3) respiratory rate greater than 25/min; and (4) presence of severe atelectasis or pulmonary edema. A bilevel positive airway pressure ventilator was used with the pressure level adjusted to minimize patient discomfort. In patients who were not able to tolerate NPPV, it was discontinued. However, it was continued until patients no longer had dyspnea without NPPV or to resolution of the initial indication for NPPV such as hypoxemia, hypercapnia, or atelectasis. Of 36 patients who underwent liver transplantation between 2005 and 2007, NPPV was administered in 6 according to our criteria. After extubation, recipients demonstrated hypoxemia, hypercapnia, tachypnea, severe atelectasis, or pulmonary edema. After treatment, these conditions improved without apparent problems related to treatment with NPPV. In 1 patient, reintubation was required because of deterioration of respiratory function due to systemic infection. In conclusion, NPPV was useful in liver transplant recipients after extubation to prevent respiratory deterioration. For successful NPPV, settings must be individualized for each patient.

RESPIRATORY COMPLICATIONS are an important cause of illness in liver transplant recipients and contribute substantially to mortality. Several studies have reported a high incidence (64.0%–84.7%) of respiratory complications after liver transplantation.[1–4] Noninvasive positive pressure ventilation (NPPV) is indicated for management not only of chronic obstructive pulmonary disease but also of acute respiratory failure to avert endotracheal

From the Department of Transplant Surgery, Nagoya University Hospital, Nagoya City, Aichi, Japan.

Address reprint requests to Prof. Shunji Nagai, Department of Transplant Surgery, Nagoya University Hospital, 65 Tsurumai, Showa-ku, Nagoya City, Aichi 466-8560, Japan. E-mail: snagai@med.nagoya-u.ac.jp

360 Park Avenue South, New York, NY 10010-1710

0041-1345/09/$–see front matter
doi:10.1016/j.transproceed.2009.06.218

Transplantation Proceedings, 41, 3919–3922 (2009)

Table 1. Clinical Causes and Outcome of NPPV Treatment

Patient, Sex, and Age	MELD Score	Primary Disease	Pretreatment Parameters (postexubation)				
			P/F Ratio	$Paco_2$, mm Hg	RR/min	Atelectasis	Pulmonary Edema
1, F, 50	20	HBV	290	48	14	Moderate	Negative
2, M, 50	19	HCV	310	47	20	Slight	Positive
3, F, 49	18	PBC	330	43	18	Severe	Negative
4, M, 58	12	HCV HCC	240	52	20	None	Negative
5, M, 58	7	HCV HCC	140	42	20	Moderate	Negative
6, F, 58	30	PBC	190	45	30	Moderate	Negative

EPAP, expiratory positive airway pressure; HBV, hepatitis B virus; HCC, hepatitis C cirrhosis; HCV, hepatitis C virus; ICU, intensive care unit; IPAP, inspiratory positive airway pressure; MELD, Model for End-Stage Liver Disease; NPPV, noninvasive positive pressure ventilation; PBC, primary biliary cirrhosis; P/F, arterial oxygen tension to fraction of inspired oxygen ratio; RR, respiratory rate; S/T, spontaneous/timed; T, timed.

Later, reintubation for mechanical ventilation was necessary because of secondary respiratory failure due to sepsis caused by an infected intra-abdominal hematoma.

*Data are given as mean (range).

†Hypoxemia due to pulmonary edema was not observed during NPPV treatment.

intubation, which is one of the most important predisposing factors for bacterial pneumonia.[5–10] Noninvasive positive pressure ventilation is delivery of assisted mechanical ventilation without the need for an invasive artificial airway.[10–12] Recently, NPPV has been used in immunocompromised patients with pneumonia and respiratory failure, with a substantial reduction in serious complications and improvement of survival rates.[13] Herein, we report our initial use of criteria-based NPPV in liver transplant recipients with respiratory compromise after extubation.

PATIENTS AND METHODS

We initiated NPPV management in 2005. Between 2005 and 2007, 36 adult patients underwent liver transplantation at our hospital. Patients who fulfilled our criteria were selected to receive NPPV.

Standard operative techniques and perioperative management were used in all patients. The immunosuppression regimens included steroids and tacrolimus or cyclosporine as a calcineurin inhibitor. Prophylactic antibiotic therapy with ampicillin and cefotaxime was administered for the first 48 hours after surgery in all patients but 1 with spontaneous bacterial peritonitis who received ampicillin and cefotaxime before the operation until his condition became stable. Chest radiography was performed daily, and 2 respiratory physicians and 2 transplant surgeons independently evaluated the radiographs for evidence of atelectasis, pulmonary edema, or pneumonia.

After extubation, respiratory function was carefully observed. Noninvasive positive pressure ventilation was applied on the basis of our criteria, as follows: (1) arterial oxygen tension to fraction of inspired oxygen ratio (P/F ratio) less than 300 and arterial carbon dioxide tension ($Paco_2$) greater than 45 mm Hg; (2) P/F ratio less than 200; (3) respiratory rate greater than 25/min; and (4) presence of severe atelectasis or pulmonary edema. Evaluation of atelectasis was based on the classification of Golfieri et al.[2] To evaluate the efficacy of treatment with NPPV, arterial oxyhemoglobin saturation (Spo_2) was continuously monitored and arterial blood gases frequently measured.

A bilevel positive airway pressure ventilator (NIP Nasal A; Teijin Ltd, Tokyo, Japan) was used in the spontaneous/timed or timed mode, which are almost equivalent to the synchronized intermittent mandatory ventilation mode or the intermittent mandatory ventilation mode, respectively. Noninvasive positive pressure ventilation was delivered through a nasal tube or appropriately sized full-face mask secured using head straps. The respiratory rate was 12/min to 14/min. The level of inspiratory positive airway pressure, defined as actual inspiratory pressure and not the pressure added to positive end-expiratory pressure, was adjusted to 7 cm/H_2O with positive expiratory airway pressure, which was equivalent to positive end-expiratory pressure of 3 cm/H_2O. Daily periods of NPPV were at least 3 hours, with use prolonged as long as possible under careful observation. Treatment with NPPV was continued until patients no longer demonstrated dyspnea without NPPV or to resolution of the initial indication for NPPV such as hypoxemia, hypercapnia, or atelectasis.

Six patients fulfilled our criteria for NPPV. Patient data are given in Table 1.

CASE REPORTS

Case 1

A 50-year-old woman with hepatitis B cirrhosis received an ABO-identical right-sided liver graft. Extubation was performed on postoperative day (POD) 3; however, hypoxemia developed on POD 4, which was an indication for treatment with NPPV. With NPPV, the hypoxemia immediately improved, and Spo_2 was maintained at 99% to 100% during treatment. Respiratory function became stable without NPPV on POD 23, and treatment was discontinued successfully.

Case 2

A 50-year-old man with hepatitis C cirrhosis received an ABO-identical whole liver graft. Although extubation was performed on POD 8, a chest radiograph demonstrated pulmonary edema, and NPPV was started. During treatment with NPPV, respiratory function was stable, and the pulmonary edema improved. However, reintubation was required on POD 18 because of septic shock due to an infected intra-abdominal hematoma. Although respiratory function was stabilized with NPPV, the treatment failed to prevent deterioration caused by the systemic infection. A second operation

Table 1. (continued)

	NPPV Treatment						Postoperative Course		
Indication	Duration, hr/d; No. of Days*	Mode	IPAP, cm H_2O	EPAP, cm H_2O	Intolerance	Outcome	Intubation Duration, d	ICU Stay, d	Respiratory Complication after NPPV Treatment
Hypoxemia and hypercapnia	5 (3–10); 20	S/T	8.0	4.0	None	Improved	3	4	None
Pulmonary edema and hypercapnia	6 (3–11); 11	S/T	7.6	3.0	None	Improved	8	9	Reintubation†
Severe atelectasis	6 (3–11); 13	S/T	7.0	4.0	None	Improved	2	3	None
Hypoxemia and hypercapnia	6 (3–11); 4	S/T	7.0	4.0	None	Improved	2	3	None
Hypoxemia	7 (4–10); 25	S/T	7.0	3.0	None	Improved	2	3	None
Hypoxemia and tachypnea	6.5 (4–12); 8	T	6.6	3.0	None	Improved	2	3	None

was performed on POD 22 to remove the infected hematoma. After the second extubation, NPPV was not used because respiratory function was stable and the patient did not meet our criteria.

Case 3

A 49-year-old woman with primary biliary cirrhosis received an ABO-identical right-sided liver graft. After extubation, chest radiographs revealed severe atelectasis in the right lower lobe. Treatment with NPPV was started on POD 3. Subsequently, the atelectasis resolved, and NPPV was discontinued.

Case 4

A 58-year-old man with hepatitis C cirrhosis and hepatic cell carcinoma received an ABO-identical right-sided liver graft. After extubation, $Paco_2$ was 52 torr, and NPPV was started on POD 5. After treatment with NPPV, $Paco_2$ decreased to 44 torr.

Case 5

A 58-year-old man with hepatitis C cirrhosis and hepatic cell carcinoma received an ABO-compatible right-sided liver graft. After extubation, severe hypoxemia developed, and a chest radiograph demonstrated moderate atelectasis. The P/F ratio was less than 20, indicating the need for treatment with NPPV, which was started on POD 10. After NPPV treatment, the Spo_2 was maintained at 99% to 100%, and the patient's condition became stable without NPPV.

Case 6

A 58-year-old woman with primary biliary cirrhosis received an ABO-compatible right-sided liver graft at emergency transplantation. After extubation, tachypnea and hypoxemia developed, and treatment with NPPV was started on POD 3. After treatment, the respiratory rate decreased from 26/min to 14/min, and Spo_2 was maintained at 100%.

RESULTS

Respiratory complications after extubation were improved in all 6 patients with NPPV treatment. All patients tolerated use of NPPV. No complications related to NPPV were observed, such as skin necrosis from an inappropriate-size mask or pneumothorax. Median (range) duration of NPPV treatment was 12 (4–25) days.

DISCUSSION

Herein, we have described the clinical utility of NPPV after liver transplantation. Treatment with NPPV provided good support for liver transplant recipients in whom respiratory function deteriorated after extubation. It is difficult to prove a direct correlation between NPPV and patient outcome. However, we observed obvious improvement in respiratory function during treatment with NPPV. By using NPPV as long as possible, further acute respiratory deterioration was prevented. As a result, patients recovered from serious respiratory conditions and demonstrated improvement in other physical conditions such as liver function, renal function, and activities of daily living, enabling successful withdrawal of NPPV treatment.

To our knowledge, there are few reports of treatment with NPPV in liver transplant recipients. Although NPPV was used in these patients on average for only 5 to 7 hours a day, we believe this treatment was important in maintaining or improving respiratory function. We hypothesized that NPPV has an intermediate role between invasive mechanical ventilation and conventional oxygen therapy via face mask or nasal cannula. Noninvasive ventilation methods such as NPPV and continuous positive airway pressure delivered via a face mask can be performed using a relatively simple device with less intensive monitoring than invasive mechanical ventilation. In postoperative respiratory management, NPPV can be placed between mechanical ventilation and oxygen therapy via a mask or nasal tube.

We observed that atelectasis, hypoxemia, and hypercapnia improved with NPPV treatment. Apparently, this treatment supports postoperative transient respiratory failure and should be considered a useful procedure in liver

transplant recipients. All 6 of our patients tolerated the therapy, although each expressed discomfort at the beginning of treatment. Furthermore, no NPPV-associated complications were observed. We optimized the NPPV settings for each patient including the mode of ventilation, mask type, respiratory rate, and inspiratory and expiratory positive airway pressures. Successful treatment depends on averting NPPV intolerance. At the beginning of treatment, relatively low inspiratory and expiratory positive airway pressures are used because high pressures are more likely to cause discomfort, and mask fitting is also important to avert intolerance. It is important that patients be observed carefully during NPPV treatment and that settings be adjusted to increase the chance of successful treatment.

In conclusion, use of NPPV for a prolonged period after extubation in liver transplant recipients is associated with improved clinical and radiologic findings. The treatment improved factors associated with respiratory failure such as hypercapnia, hypoxemia, labored respiration, and atelectasis. For NPPV to be successful, it is important that settings be individualized for each patient to avert intolerance. Treatment with NPPV can contribute to more efficient respiratory management in liver transplant recipients.

REFERENCES

1. Chin K, Uemoto S, Takahashi K, et al: Noninvasive ventilation for pediatric patients including those under 1-year-old undergoing liver transplantation. Liver Transpl 11:188, 2005

2. Golfieri R, Giampalma E, Morselli Labate AM, et al: Pulmonary complications of liver transplantation: radiological appearance and statistical evaluation of risk factors in 300 cases. Eur Radiol 10:1169, 2000

3. Pirat A, Ozgur S, Torgay A, et al: Risk factors for postoperative respiratory complications in adult liver transplant recipients. Transplant Proc 36:218, 2003

4. Araz C, Pirat A, Torgay A, et al: Early postoperative complications of pediatric liver transplantation: experience at one center. Transplant Proc 36:214, 2004

5. Antonelli M, Conti M, Bufi M, et al: Noninvasive ventilation for treatment of acute respiratory failure in patients undergoing solid organ transplantation. JAMA 283:235, 2000

6. Hillbert G, Gruson D, Vargas F, et al: Noninvasive continuous positive airway pressure in neutropenic patients with acute respiratory failure requiring intensive care unit admission. Crit Care Med 28:3185, 2000

7. Hillbert G, Gruson D, Gbikpi-Benissan G, et al: Noninvasive pressure support ventilation in COPD patients with postextubation hypercapnic respiratory insufficiency. Eur Respir J 11:1349, 1998

8. Matte P, Jacquet L, Van Dyck M, et al: Effects of conventional physiotherapy, continuous positive airway pressure and non-invasive ventilatory support with bilevel positive airway pressure after coronary artery bypass grafting. Acta Anaesthesiol Scand 44:75, 2000

9. Hillbert G, Gruson D, Gbikpi-Benissan G, et al: Sequential use of noninvasive pressure support ventilation for acute exacerbations of COPD. Intens Care Med 23:955, 1997

10. Sangeeta M, Gregory J, Robert WH, et al: Randomized, prospective trial of bilevel versus continuous positive airway pressure in acute pulmonary edema. Crit Care Med 25:620, 1997

11. Carrey Z, Gottfried SB, Levy RD: Ventilatory muscle support in respiratory failure with nasal positive pressure ventilation. Chest 97:150, 1990

12. Liesching T, Kwok H, Hill NS: Acute applications of noninvasive positive pressure ventilation. Chest 124:699, 2003

13. Hilbert G, Gruson D, Vargas F, et al: Noninvasive ventilation in immunosuppressed patients with pulmonary infiltrates, fever, and acute respiratory failure. N Engl J Med 344:481, 2001

REGENERATION AND TRANSPLANTATION NEUROREPORT

CD133$^+$ cells from human peripheral blood promote corticospinal axon regeneration

Risako Yamamoto[a], Masakazu Ishikawa[a], Nobuhiro Tanaka[a], Naosuke Kamei[a], Kazuyoshi Nakanishi[a], Hirofumi Sasaki[a], Toshio Nakamae[a], Yu Mochizuki[a], Takayuki Asahara[b] and Mitsuo Ochi[a]

[a]Department of Orthopaedic Surgery, Graduate School of Biomedical Sciences, Hiroshima University and [b]Tokai University School of Medicine, Kanagawa, Japan

Correspondence to Risako Yamamoto, MD, 1-2-3 Kasumi, Minami-ku, Hiroshima City, Hiroshima, 734-8551, Japan
Tel: +81 82 257 5233; fax: +81 82 257 5234; e-mail: riyamamoto@hiroshima-u.ac.jp

Received 28 February 2008; accepted 2 March 2008

To assess the effect of endothelial progenitor cells on the axon growth of cortex neurons, we transplanted CD133$^+$ cells derived from human peripheral blood to an organotypic coculture system consisting of spinal cord and cortex from neonatal rats. The axon growth from cortex to spinal cord was significantly promoted in cultures after CD133$^+$ cells transplantation compared with that of the control cultures. In addition, real-time reverse transcription-PCR showed a significant upregulation of vascular endothelial growth factor mRNA in the spinal cord of the cultures containing CD133$^+$ cells. In contrast, the transplanted cells did not differentiate into endothelial cells. These data suggest that CD133$^+$ cells may promote axonal regeneration by upregulating vascular endothelial growth factor mRNA in spinal cord tissues. *NeuroReport* 19:799–803 © 2008 Wolters Kluwer Health | Lippincott Williams & Wilkins.

Keywords: axonal regeneration, CD133, cell transplantation, corticospinal tract, human peripheral blood, slice culture, vascular endothelial growth factor

Introduction

Treatments that enhance the regeneration of damaged axons in the central nervous system (CNS) have a potential for improving recovery after spinal cord injury (SCI). Cell transplantation, using neural stem/progenitor cells (NPCs) or bone marrow stromal cells (MSCs), is a promising therapeutic approach for treating SCI [1–3]. Asahara *et al.* [4] reported the isolation of putative endothelial progenitor cells (EPCs) in a population of CD34$^+$ cells obtained from human peripheral blood. CD133 is the best selective marker for identifying EPCs [5]. CD133$^+$ cells are able to differentiate into several phenotypes including astrocytes, neurons [6], and endothelial cells (ECs) [7]. ECs contribute to self-renewal of NPCs or neurogenesis [8]. Therefore, the transplantation of EPCs may be beneficial in regeneration in the CNS.

Angiogenesis and neurogenesis are prominent features of neurological disease, and many commonalities between these processes have been identified [9]. A growth factor shared by these events is vascular endothelial growth factor (VEGF). VEGF promotes the growth of neuronal processes [10], stimulates the proliferation of neuronal precursors [11], and protects neurons from injuries [12].

from human peripheral blood on corticospinal axon growth and the mechanism of the axonal regeneration using the organotypic coculture system.

Material and methods

Our research methods were reviewed and approved by the ethical committee of Hiroshima University.

Isolation and preparation of human CD133$^+$ cells

Informed consent was obtained from all participants. Total peripheral blood mononuclear cells from healthy adults were isolated from 200 ml of fresh blood by Histopaque 1077 (Sigma-Aldrich, Oakville, Canada) density-gradient centrifugation of buffy coats. CD133$^+$ cells were separated from peripheral blood mononuclear cells using CD133-bound microbeads and a magnetically activated cell sorter (autoMACS; Miltenyi Biotec, Bergisch-Gladback, Germany) following the manufacturer's protocol. Using the harvested enriched CD133$^+$ cell sample, cytometric analyses were performed using a FACScalibur flow cytometer and Cell Quest software (BD PharMingen, San Diego, California, USA). The isolated cells showed 62–72% purity for

REJUVENATION RESEARCH
Volume 11, Number 2, 2008

DOI: 10.1089/rej.2008.0668

Characterizing Endothelial Cells Derived from the Murine Embryonic Stem Cell Line CCE

Fardin Fathi,[1] Abbas Jafari Kermani,[2] Leila Pirmoradi,[3] Seyed Javad Mowla,[2] and Takayuki Asahara[4]

ABSTRACT

Embryonic stem cells (ESC) are defined by two main properties of self-renewal and their multipotency to differentiate into virtually all cell types of the body, including endothelial cells. ESCs have been widely regarded as an unlimited source of cells in regeneration medicine and also an ideal *in vitro* model to investigate complex developmental processes. Here, we report a simple and efficient *in vitro* model to derive a nearly pure population of endothelial cells from a murine ESC line. CCE ES cells are exposed to alpha-MEM medium containing 10% FBS for 4 days and then cultured in endothelial basal-2 medium containing vascular endothelial growth factor (VEGF), basic fibroblast growth factor (bFGF), insulin-like growth factor (IGF), epidermal growth factor (EGF), and 2% FBS for 42 days. The cells acquired a relatively uniform endothelial cell morphology and were able to propagate and expand in culture. When murine ES cell–derived endothelial cells (MESDECs) were cultured on Matrigel and incubated for 48 h, vessel-like tube structures consisting of CD31 (PECAM-1) or BS-1 immunoreactive cells were developed. Immunocytochemistry and RT-PCR analyses revealed that MESDECs express endothelial cell-specific marker proteins such as Flk-1, PECAM-1, Tie-1, and Tie-2, in which the expressions persist for long periods of time after differentiation. The cells were also capable of taking up acetylated low-density lipoprotein (LDL) in culture. Our data suggest that MESDECs could provide a suitable *in vitro* model to study molecular events involved in vascular development and open up a new therapeutic strategy in regeneration medicine of cardiovascular disorders.

INTRODUCTION

EMBRYONIC STEM (ES) CELLS are defined by two main properties of self-renewal and their ability to differentiate into virtually all cell types of the body, spontaneously or under the influence of inductive agents.[1] While these cells are primarily considered promising cell sources for regeneration medicine, they also provide a simple and controllable system to investigate complex developmental processes *in vitro*. ES cells can be maintained in their pluripotential state in the presence of leukemia inhibitory factor (LIF), which inhibits their differentiation. Upon removal of LIF, ES cells spontaneously differentiate into cyst-like structures, termed *embryoid bodies* (EB), which contain derivatives of all three primitive germ layers.[2]

Among various differentiated cell types derived from EBs, there are blood island-like structures that consist of immature hemato-

[1]KDRC, Faculty of Medicine, Kurdistan University of Medical Sciences, Sanandaj, Iran.
[2]Department of Genetics, Faculty of Basic Sciences, Tarbiat Modares University, Tehran, Iran.
[3]Department of Physiology, Faculty of Medicine, Kurdistan University of Medical Sciences, Sanandaj, Iran.
[4]Group of Vascular Research, Kobe Institute of Biomedical Research and Innovation/Riken Center for Developmental Biology, Chuo-Ku, Kobe, Japan.

poietic cells surrounded by endothelial cells, along with vascular-like channels on the surface of EBs.[2] The later observation suggests that ES cells produce all factors, which are necessary for proper induction of vasculogenesis.[2] The induction of *in vitro* vasculogenesis from ES cells normally required formation of embryoid bodies[2–6] and this has largely restricted identification of cellular intermediates between mesodermal cells and committed precursors for hematopoietic and endothelial cell lineages.[7]

In this study, we used a murine ES cell line (CCE) to investigate the induction potential of EGM2 medium to induce endothelial cell differentiation. We were able to differentiate CCE cells into Flk-1 positive cells using the method reported by Nishikawa et al.[8] and then induced endothelial differentiation of Flk-1 positive cells by using EGM2 medium. Our data reveal that EGM2 medium, which has defined growth factors known to support endothelial cell growth, is capable of driving a homogenous population of endothelial-appearing cells from Flk-1 positive cells. The state of differentiation of ESC-derived endothelial cells was then investigated with RT-PCR and immunocytochemistry techniques.

MATERIALS AND METHODS

CCE culture and induction of endothelial cell differentiation

CCE ES cells[8,9] were cultured in Dulbecco modified essential medium (DMEM, Gibco, Paisley, United Kingdom) containing 15% fetal bovine calf serum (FBS, Gibco), 10 ng/mL leukemia inhibitory factor (LIF, Sigma, St. Louis, MO), and 5×10^{-5} M 2-mercaptoethanol (2ME, Sigma). 1×10^4 ES cells were then transferred to each well of 6-well dishes (Becton-Dickinson, Oxnard, CA) precoated with type IV collagen (C5533, Sigma) and incubated in a-MEM (Gibco), supplemented with 10% FBS and 5×10^{-5} M 2ME. Although no exogenous growth factors were added, a more than 100-fold increase of cells was observed during a 4-day incubation. To induced endothelial cell differentiation, cultured cells were harvested in day 4, and were put into a 6-well plate that was precoated with fibronectin (F2006, Sigma) and incubated in endothelial cell basal medium-2 (EBM2, Clonetics Cambrex, Wokingham, United Kingdom) containing 2% FBS, vascular endothelial growth factor (VEGF), basic fibroblast growth factor (bFGF), insulin-like growth factor 1 (IGF-1), epidermal growth factor (EGF), and ascorbic acid (EGM2-MV Bullet Kit; Clonetics). The Flk-1 positive cells were differentiated for 4 weeks in the EGM2 medium, which was changed every 3 to 5 days. Differentiated cells were dissociated with 0.25% trypsin/EDTA (ethylene diamine tetraacetic acid; Gibco) for 2 min, centrifuged, and replated in EGM2 in 6-cm tissue culture dishes precoated with fibronectin. After 24 h, non-adherent cells were removed and adherent cells were fed with fresh medium. The murine ESC-derived endothelial cells (MESDECs) could be grown to confluence and expanded in the EGM2 medium. Theses cells were passaged every 3 to 5 days for up to 10 times. In days 0, 4, 18, 32, and 46, the cells were harvested and analyzed for expression of endothelial cell markers by RT-PCR and immunocytochemistery techniques.

Induction of tube formation on Matrigel

Matrigel (Sigma) was added to each well of a 4-well culture slide and allowed to solidify at 37°C for at least 30 min under a laminar hood. Then, 0.5 mL of a cell suspension containing around 4×10^5 to 1×10^5 MESDECs was placed on top of the Matrigel. The cultures were incubated at 37°C and 5% CO_2, and observed at 24 and 48 h for rearrangement of cells into capillary-like structures.

Antibodies

Anti-PECAM-1 (MEC 13.3) is a rat monoclonal antibody raised against 129/Sv murine-derived endothelioma cell line, tEnd.1. Anti-VE-cadherin (C-19) is an affinity-purified goat polyclonal antibody raised against peptides mapped at the carboxy terminus of VE-cadherin of human origin (Santa Cruz Biotechnology, Santa Cruz, CA). A donkey TR-conjugated anti-goat IgG and a goat FITC-conjugated anti-rat IgG secondary antibody (Santa Cruz Biotechnology) were used.

Dil uptake staining

Cultured cells were incubated in EGM2 supplemented with 2% FBS and 10 μg/mL Dil-Ac-LDL (Biomedical Technologies, Stoughton, MA) for 4 h. Cells were then washed with fresh EGM2 and observed by fluorescent microscopy (TE-300, Nikon, Tokyo, Japan) using a Texas-RED filter.

Immunocytochemistry

Cells grown on 4-well culture slides were washed with phosphate-buffered saline (PBS) for 3 min and fixed in 4% paraformaldehyde (Merck, Darmstadt, Germany) for 20 min. Then, the cells were rinsed in PBS, and stored in PBS at 4°C until required. All steps of fixation, permeabilization, washing, and incubation with antibodies were performed at room temperature. The fixed cells were permeabilized for 15 min in PBS containing 0.02% Triton X-100 (Sigma), blocked for 60 min in PBS-Triton X-100 containing 10% serum and 0.02% Triton X-100, and incubated with first antibodies against CD31 (1:100) for 120 min at 37°C and with a VE-cadherin (1:50–1:1000) for 120 min at 37°C or 4°C overnight. The samples were then incubated for 60 min with TR (1:100) or FITC (1:100)-conjugated secondary antibodies against CD31 and VE-cadherin antibodies, respectively. For double-labeled immunofluorescent, the fixed cells were incubated with BS-1 lectin for 1 h in room temperature, then with primary antibody against CD31, and then secondary antibody conjugated with TR. PBS Triton X-100 blocking with 2% serum was used for washing the specimens between incubations and diluting the antibodies. Cover slips were mounted in Vectashield Hard+Set mounting medium containing DAPI (Vector Laboratories, Burlingame, CA) and immediately examined under a fluorescent microscope.

RT-PCR analysis

Total RNA was isolated from the differentiated cells using an RNA purification kit (Sinagen, Iran). One μg of total RNA was reverse transcribed into DNA using AMV reverse transcriptase and oligo (dT) primer (Bionner, Cheongwon, South Korea). RT-PCR was performed in a 50 μL reaction mixture using a thermal cycler (Mastercycler, Eppendorf, Hamburg, Germany). Aliquots of 4 μL of cDNA were then subjected to PCR amplification using a PCR kit (Bionner) and primer sets that were specific to the genes of interest (Table 1). The PCR conditions were initial denaturation for 5 min at 94°C followed by 35 cycles of denaturation for 45 s at 94°C, annealing for 45 s at 60–65°C (depending on primers) and extension for 60 s at 72°C. The reaction was followed by a final extension step of 5 min at 72°C. The expression of GAPDH mRNA, a constitutively and ubiquitously expressed gene, served as an internal control in all RT-PCR reactions.

TABLE 1. SEQUENCE OF PRIMERS AND PCR CONDITIONS TO AMPLIFY SELECTED GENES

Genes	*Length (bp)*	*Primer sequences (5′ ≥ 3′)*	*Annealing temperature (°C)*
CD31	261	GTCATGGCCATGGTCGAGTA CTCCTCGGCATCTTGCTGAA	63
Flk-1	530	AAGGTGCCCAGGAAAAGAC CTTGCCCCGTAAGTAAGTTG	64
VE-cadherin	457	GGCTTTCTGACTGTTGTGGAC TTATAGATGTTTCCCTGCTTGG	64
CD34	682	GCAGCTTTGAGATGACATCACCCAC CTTGCTGAATGGCCGTTTCTGGAAG	65
Tie-1	514	TGATGGCGAATGTGTGTGTC AAACTCTGCTGTGGTCCTGTC	64
Tie-2	633	TGGAATGACTTGCATCACCGTGCTG GCCAGGTCCCTGTGGATAAACTGTT	64
GAPDH	308	GCCCATCACCATCTTCCAG TGAGCCCTTCCACAATGCC	64

RESULTS

Derivation of endothelial-like cells from CCE cell line

CCE ES cells that were maintained in a gelatin-coated dish in the presence of LIF were transferred into a type IV collagen-coated dish and cultured in the absence of LIF to induce their differentiation toward mesodermal cell lineage. A more than 100-fold increase in the number of cells was observed during a 4-day incubation time. The cells harvested and the expression of fetal liver kinase-1 (Flk-1) gene, a tyrosine kinase receptor for vascular endothelial growth factor (VEGF), was analyzed with RT-PCR. To induce endothelial cell differentiation, the Flk-1$^+$ cells were cultured in fibronectin-coated dishes in the presence of EGM2 medium containing VEGF, bFGF, EGF, and IGF (as described in the Materials and Methods section). After 2 weeks, the cells assumed a uniform morphology similar to the elongated endothelial cells (Fig. 1A). The endothelial-like cells were serially passaged and expanded up to 10 population doublings in EGM2 medium. After 4 weeks, the cells displayed a cobblestone-like morphology (Fig. 1C). In contrast, CCE cells grown in medium supplemented with FBS alone differentiated into a heterogeneous cell population with no distinct endothelial-appearing morphology.

To further test the identity of differentiated cells, the cells were cultured in Matrigel-based media, where they rapidly formed capillary-like (Fig. 1B) and network-like structures (Fig. 1D). The latter morphological changes were observed within 48 h after plating the endothelial-l cells in days 18 and 32 of the experiment, respectively.

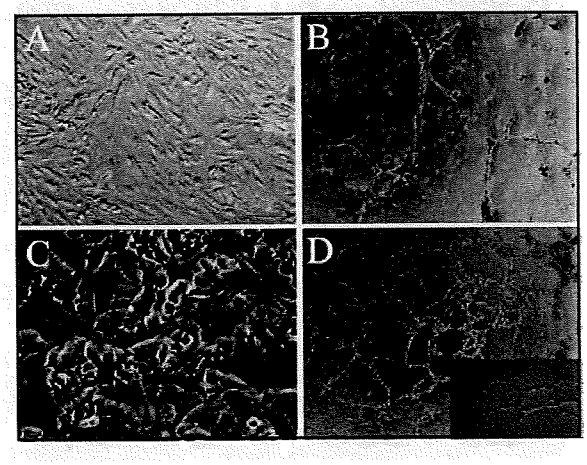

FIG. 1. Phase-contrast microscopy of the morphology of the Flk-1$^+$ CCE cell–derived endothelial-like cells in culture. The cells were grown in EGM2 media and on fibronectin precoated plates. **(A)** After 2 weeks, the cells were transferred to a new tissue culture plate, where uniform, adherent, fusiform cells were evident. **(C)** After 4 weeks, the cells displayed a cobblestone-like morphology. MESDECs were made into a single-cell suspension and transferred to a Matrigel-coated plate where cord-like structures **(B)** and network formation **(D)** were observed 48 h after plating in days 18 and 32 of the experiment, respectively. Original magnifications, ×200 **(A and C)**; ×100 **(B and D)**.

Characterizing the identity of murine ES cell-derived endothelial-like cells

To evaluate how closely the CCE-differentiated cells mimic the phenotype of endothelial cells, the potential expression of several endothelial-specific genes was analyzed before and after the induction of differentiation in the cells (Fig. 2). The RT-PCR result demonstrates the expression of Flk-1 gene in all time courses after differentiation, with no expression in undifferentiated cells. In contrast, the expression of another endothelial marker, CD31 (platelet endothelial cell adhesion molecule-1), begins at 18 days after the induction of differentiation and remains almost unchanged thereafter. Tie-1 and Tie-2, two related receptor tyrosine kinases that are expressed predominantly in endothelial cells, were expressed much later in the course of differentiation, while Tie-2 and Tie-1 expression was detected at 32 and 46 days after the induction of differentiated, respectively. In contrast, there was no expression for vascular endothelial cadherin (VE-cadherin, a key endothelial cell adhesion molecule) and CD34 genes, another endothelial cell marker, in all of the examined time courses.

Our immunostaining data further reveal that the CCE–derived endothelial-like cells have the ability to rapidly take up acetylated LDL (acLDL) (Fig. 3C) and to bind it to BS-1 lectin (Fig. 3B and D). We also analyzed the potential expression of CD31 and VE-cadherin proteins in Flk-1$^+$ CCE cell-derived endothelial-like cells in culture on day 32. The differentiated en-

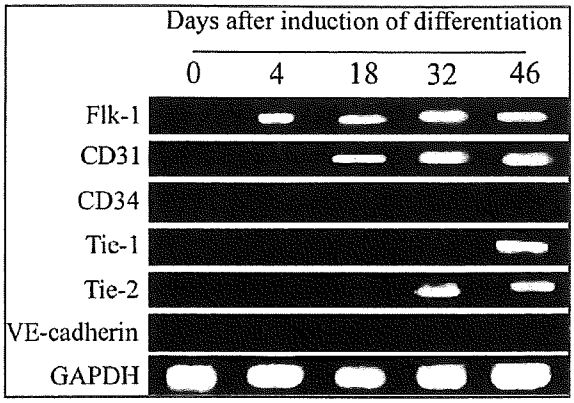

FIG. 2. Expression of endothelial specific genes Flk-1, CD31, CD34, Tie-1, Tie-2, and VE-cadherin in murine CCE ES cells before and during endothelial differentiation. The cells exposed to alpha-MEM medium containing 10% FBS for 4 days and then cultured in EGM2 medium supplemented with 2% FBS for 42 days. Day 0 represents undifferentiated cells and day 4 corresponds to the last day of culture in alpha-MEM medium. Days 18, 32, and 46 of experiment are the continuation of cell culturing in EGM2 medium. All amplifications were performed for 35 cycles. As the data show, no signal was detected for CD34 and VE-cadherin genes, neither before nor after differentiation. For other genes, the expression was evident only after a long period of time after differentiation. The expression of GAPDH was monitored in all experiments as an internal control.

dothelial cells stained positively for CD31 (Fig. 2A), whereas there was no immunostaining signal for VE-cadherin. Figure 2D shows the subcellular distribution of CD31 and BS-1 lectin in the same CCE-derived vascular-like structures.

DISCUSSION

In the present report, we provide further *in vitro* evidence that murine ES cells can differentiate into endothelial lineage, ultimately forming vascular structures on Matrigel. We also describe the derivation of a nearly pure population of endothelial cells from a murine ES cell line, CCE. The identity of the differentiated cells was then analyzed based on their morphology, cell surface antigens, expression of endothelial-specific genes, binding to BS-1 lectin, and uptake of acetylated LDL. Moreover, when differentiated cells were cultured on Matrigel, they were able to form cord-like/tube structures mimicking the structure of blood vessels.

So far several *in vitro* systems have been developed for investigating the cellular and molecular events of vasculogenesis. One of the most popular systems employs ESC-derived embryoid body and culturing of mesodermal cells from embryos.[10–13] Although these culture systems provide a simple means to investigate *in vitro* vasculogenesis, the existence of many other lineage cells generated in an uncontrollable manner hinders a good understanding of the events occurring during endothelial cell (EC) differentiation.[10]

Hirashima et al. isolated Flk-1$^+$ EC progenitors derived from ES cells and then differentiated purified Flk-1$^+$ cells into ECs by using type IV collagen coated dishes. Despite providing a new tool to produce EC progenitors from murine ES cells, their culture system was still insufficient to induce the formation of tubular networks.[10] Also, in Ogawa et al.'s coculture system for endothelial differentiation of Flk-1$^+$ cells, the percentage of cells capable of forming endothelial cell colony was only 3%.[7] In contrast, the method or cell line that we used

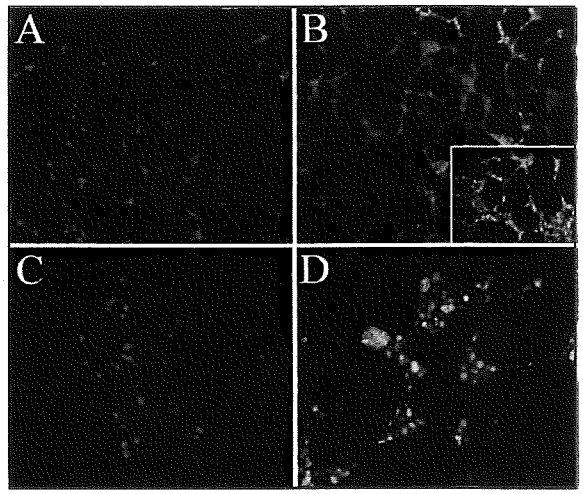

FIG. 3. Representative immunocytochemistry data of endothelial-specific protein expression in MESDECs. The cells were grown on culture slides precoated with fibronectin and were analyzed for the presence of PECAM-1, VE-cadherin, and BS-1 lectin proteins or for the uptake of acetylated LDL by the cells. The result shows a positive staining signal for PECAM-1 **(A)** and BS-1 lectin **(B)**. **(C)** The result also demonstrates the uptake of acetylated LDL by MESDECs. **(D)** MESDECs grown as tubes in Matrigel and double-stained for PECAM-1 and BS-1 lectin; cell nuclei were counterstained with DAPI. Magnification, ×100 (day 32).

to derive endothelial cells is unique in that virtually all cells have the same endothelial phenotype based on their surface antigen expression. Our method also promoted active vessel formation when the cells were uniformly suspended on a Matrigel.

Kaufman et al. reported that culturing monkey ES cells in EGM2 medium generated a homogenous population of endothelial-appearing cells.[14] These cells expressed many cell surface antigens and endothelial-specific genes similar to the endothelial cells isolated from other sources. Moreover, these cells are shown to produce functional blood vessels, which contribute directly to angiogenesis of tumor implants. Interestingly, undifferentiated rhesus monkey ES cells are Flk-1^+.[14] Therefore, growth of these cells in media containing VEGF may directly promote the induction of endothelial cells differentiation. Consistently, our data demonstrate that EGM2 medium is able to stimulate the derivation of endothelial cells from the murine ES cell line CCE.

During *in vivo* and *in vitro* vasculogenesis, Flk-l is the earliest endothelial marker being expressed in both extra-embryonic and embryonic mesoderm at E7.0.[1,15,16] Our finding that the expression of Flk-1 proceeds that of other endothelial-specific genes is in agreement with the mentioned reports and further supports the idea that Flk-1 binding by its ligand, VEGF, can initiate the induction of endothelial cell differentiation. CD31 was the next to be expressed following the expression of Flk-1. This finding is in agreement with the onset of its expression *in vivo* at E7.0 to E7.5, when the yolk sac vasculature will appear. The onset of Tie-2 and Tie-1 expression begins later than that of Flk-1 and CD31. A detailed study on the developmentally expression profiles of Flk-1, Tie-2, and Tie-1 have already shown that these molecules are sequentially expressed at 0.5 day intervals from E7.0 to E8.0. Thereafter, the sequential expression pattern of these markers in our experiment seems to be well fitted with their real sequential expression during development.[1,16–18]

Our data reveal that the endothelially differentiated CCE cells bind BS-1 lectin, uptake acetylated LDL, and express endothelial-specific genes CD31, Tie-1, Tie-2, and Flk-1. However, the absence of CD34 and VE-cadherin expression in the cells suggest that we have probably obtained a new subpopulation of endothelial-like cells. Accordingly, various studies have characterized subpopulations of endothelial cells lacking CD34 and/or VE-cadherin expression.[14,19,20] Moreover, the expression of these surface antigens is not unique to endothelial cells and both genes can be expressed in hematopoietic precursor cells.[21–24] Also, the expression of VE-cadherin can be detected on some aggressive melanoma.[25]

ES cell–derived endothelial cells could have some clinical usefulness in re-vasculogenesis of ischemic tissues. Based on previous studies, endothelial cells derived from murine and monkey ES cells can form functional vasculature *in vivo*.[14,26] Furthermore, peripheral blood of adults contains a subtype of circulating, bone-marrow-derived cells with properties similar to those of embryonal angioblasts. These cells have the potential to proliferate and differentiate into mature endothelial cells and therefore were termed *endothelial progenitor (precursor) cells* (EPC).[27] Recent studies[28–30] in animals and human suggest the ability of EPCs to improve the function of ischemic organs, possibly by both induction and modulation of vasculogenesis and angiogenesis in areas with reduced oxygen supply or by stimulating the re-endothelialization of injured vessels.[31] Other progenitor cells isolated from human bone marrow form endothelial cells that contribute to regions of active angiogenesis.[32] Since ES cells can be grown in virtually unlimited numbers, these cells may serve as an unlimited source of therapeutic endothelial cells.[14]

In conclusion, our data reveal that the treatment of murine ESC-derived Flk-1^+ cells with defined growth factors known to support endothelial cell growth leads to the generation of a homogenous population of immortalized endothelial-like cells, which could be a source of endothelial cells for therapeutic applications. On the other hand, understanding the molecular aspects of vasculogenesis could provide a new strategy to combat the growth of tumors.

ACKNOWLEDGMENTS

This work was supported by a research grant from the Kurdistan University of Medical Sciences.

REFERENCES

1. Robertson EJ. Teratocarcinoma and Embryonic Stem Cells: A Practical Approach. Oxford: IRL Press, 1987.
2. Vittet D, Prandini MH, Berthier R, Schweitzer A, Sisterno H, Uzan G, et al. Embryonic stem cells differentiate in vitro to endothelial cells through successive maturation steps. Blood 1996;88:3424–3431.
3. Burkert U, von Ruden T, Wagner, EF. Early fetal hemopoietic development from in vitro differentiated embryonic stem cells. New Biol 1991;3:698–708.
4. Wiles MV, Keller G. Multiple hematopoietic lineages develop from embryonic stem (ES) cells in culture. Development 1991;111:259–267.
5. Wang R, Clark R, Bautch VL. Embryonic stem cell-derived cystic embryoid bodies form vascular channels: an in vitro model of blood vessel development. Development 1992;114:303–316.
6. Doetschman T, Shull M, Kier A, Coffin JD. Embryonic stem cell model systems for vascular morphogenesis and cardiac disorders. Hypertension 1993;22:618–622.
7. Ogawa M, Kizumoto M, Nishikawa S, Fujimoto T, Kodama H, Nishikawa SH. Expression of a4-integrin defines the earliest precursor of hematopoietic cell lineage diverged from endothelial cells. Blood 1999;93: 1168–1177.
8. Nishikawa SI, Nishikawa S, Hirashima M, Matsuyoshi N, Kodama H. Progressive lineage analysis by cell sorting and culture identifies $FLK1^+$ $VEcadherin^+$ cells at a diverging point of endothelial and hemopoietic lineages. Development 1998;125:1747–1757.
9. Fathi F, Altiraihi T, Mowla SJ, Movahedin M. Transfection of CCE mouse embryonic stem cells with EGFP and BDNF genes by the electroporation method. Rejuvenation Res 2006;9:26–30.
10. Hirashima M, Kataoka H, Nishikawa S, Matsuyoshi N, Nishikawa SI. Maturation of embryonic stem cells into endothelial cells in an in vitro model of vasculogenesis. Blood 1999;93:1253–1263.
11. Doetschman TC, Eistetter H, Katz M, Schmidt W, Kemler R. The in vitro development of blastocyst-derived embryonic stem cell lines: formation of visceral yolk sac, blood islands and myocardium. J Embryol Exp Morphol 1985;87:27–45.
12. Palis J, McGrath KE, Kingsley PD. Initiation of hematopoiesis and vasculogenesis in murine yolk sac explants. Blood 1995;86:156–163.
13. Risau W, Sariola H, Zerwes HG, Sasse J, Ekblom P, Kemler R, et al. Vasculogenesis and angiogenesis in embryonic-stem-cell derived embryoid bodies. Development 1988;102:471–478.
14. Kaufman DS, Lewis RL, Hanson ET, Auerbach R, Plendl J, Thomson JA. Functional endothelial cells derived from rhesus monkey embryonic stem cells. Blood 2004;103:1325–1332.
15. Yamaguchi TP, Dumont DJ, Conlon RA, Breitman ML, Rossant J. Flk-1, an flt-related receptor tyrosine kinase is an early marker for endothelial cell precursors. Development 1993;118:489–498.
16. Dumont DJ, Fong GH, Pun MC, Gradwohl G, Alitalo K, Breitman ML. Vascularization of the mouse embryo: a study of flk-1, tek, tie, and vascular endothelial growth factor expression during development. Dev Dynamics 1995;203:80–92.
17. Sat TN, Qin Y, Kozak CA, Audus KL. Tie-1 and tie-2 define another class of putative receptor tyrosine kinase genes expressed in early embryonic vascular system. Proc Natl Acad Sci USA 1993;90:9355–9358.
18. Baldwin HS, Shen HM, Yan HC, Delisser HM, Chung A, Mic Kanin C. Platelet endothelial cell adhesion molecule-1 (PECAM-1KD3 I): alternatively spliced, functionally distinct isoforms expressed during mammalian cardiovascular development. Development 1994;120:2539–2553.
19. Balconi G, Spagnuolo R, Dejana E. Development of endothelial cell lines from embryonic stem cells: a tool for studying genetically manipulated endothelial cells in vitro. Arterioscler Thromb Vasc Biol 2000;20:1443–1451.
20. Cines DB, Pollak ES, Buck CA, Loscalzo J, Zimmerman GA, McEver RP, et al. Endothelial cells in physiology and in the pathophysiology of vascular disorders. Blood 1998;91:3527–3561.
21. Watt SM, Williamson J, Genevier H, Fawcett J, Simmons DL, Hatzfeld A, et al. The heparin binding PECAM-1 adhesion molecule is expressed by CD34_ hematopoietic precursor cells with early myeloid and B-lymphoid cell phenotypes. Blood 1993;82:2649–2663.
22. Chan JY, Watt SM. Adhesion receptors on haematopoietic progenitor cells. Br J Haematol 2001;112:541–557.
23. Oberlin E, Tavian M, Blazsek I, Peault B. Blood forming potential of vascular endothelium in the human embryo. Development 2002;129:4147–4157.
24. Fraser ST, Ogawa M, Yu RT, Nishikawa S, Yoder MC, Nishikawa S. Definitive hematopoietic commitment within the embryonic vascular endothelial-cadherin(+) population. Exp Hematol 2002;30:1070–1078.
25. Hendrix MJ, Seftor EA, Meltzer PS, Gardner LM, Hess AR, Kirschmann DA, et al. Expression and functional significance of VE-cadherin in aggressive human melanoma cells: role in vasculogenic mimicry. Proc Natl Acad Sci USA 2001;98:8018–8023.
26. Yamashita J, Itoh H, Hirashima M, Ogawa M, Nishikawa S, Yurugi T, et al. Flk1-positive cells derived from embryonic stem cells serve as vascular progenitors. Nature 2000;408:92–96.
27. Asahara T, Murohara T, Sullivan A, Silver M, Zee RVZ, Li T, et al. Isolation of putative progenitor endothelial cells for angiogenesis. Science 1997;275:964–967.
28. Kocher AA, Schuster MD, Szabolcs MJ, Takuma S, Burkhoff D, Wang J, et al. Neovascularization of ischemic myocardium by human bone-marrow-derived angioblasts prevents cardiomyocyte apoptosis, reduces remodeling and improves cardiac function. Nat Med 2001;7:430–436.
29. Walter DH, Rittig K, Bahlmann FH, Kirchmair R, Silver M, Murayama T, et al. Statin therapy accelerates re-endothelialization: a novel effect involving mobilization and incorporation of bone marrow-derived endothelial progenitor cells. Circulation 2002;105:3017–3024.

30. Assmus B, Schächinger V, Teupe C, Britten M, Lehmann R, Döbert N, et al. Transplantation of progenitor cells and regeneration enhancement in acute myocardial infarction (TOPCARE-AMI). Circulation 2002;106:3009–3017.
31. Hristov M, Erl W, Weber PC. Endothelial progenitor cells, isolation and characterization. TCM 2003;13: 201–206.
32. Reyes M, Dudek A, Jahagirdar B, Koodie L, Marker PH, Verfaillie CM. Origin of endothelial progenitors in human postnatal bone marrow. J Clin Invest 2002; 109:337–346.

Address reprint requests to:
Fardin Fathi
KDRC, Faculty of Medicine
Kurdistan University of Medical Sciences
Sanandaj
Iran

E-mail: farfath@yahoo.com

This article has been cited by:

1. S. Lange, J. Heger, G. Euler, M. Wartenberg, H. M. Piper, H. Sauer. 2008. Platelet-derived growth factor BB stimulates vasculogenesis of embryonic stem cell-derived endothelial cells by calcium-mediated generation of reactive oxygen species. *Cardiovascular Research* **81**:1, 159-168. [CrossRef]

STEM CELLS®

TRANSLATIONAL AND CLINICAL RESEARCH

Local Delivery of Granulocyte Colony Stimulating Factor-Mobilized CD34-Positive Progenitor Cells Using Bioscaffold for Modality of Unhealing Bone Fracture

YUTAKA MIFUNE,[a,b] TOMOYUKI MATSUMOTO,[a,b] ATSUHIKO KAWAMOTO,[a] RYOSUKE KURODA,[b] TARO SHOJI,[a,b] HIROTO IWASAKI,[a] SANG-MO KWON,[a] MASAHIKO MIWA,[b] MASAHIRO KUROSAKA,[b] TAKAYUKI ASAHARA[a,c]

[a]Stem Cell Translational Research, Institute of Biomedical Research and Innovation/RIKEN Center for Developmental Biology, Kobe, Japan; [b]Department of Orthopedic Surgery, Kobe University Graduate School of Medicine, Kobe, Japan; [c]Department of Regenerative Medicine Science, Tokai University School of Medicine, Kanagawa, Japan

Key Words. CD34 stem cells • CD34 progenitors • CD34 cell dose • Cellular therapy • Cell transplantation • Osteoblast • Endothelial cell • Stem cell transplantation

ABSTRACT

We recently reported that i.v. transplantation of adult human circulating CD34+ cells, an endothelial/hematopoietic progenitor-enriched cell population, contributes to fracture healing through the enhancement of vasculogenesis and osteogenesis. However, the scarcity of CD34+ cells in the adult human is a critical issue for the future clinical application of this method. To overcome this issue, we assessed in vitro and in vivo capacity of granulocyte colony-stimulating factor-mobilized peripheral blood (GM-PB) human CD34+ cells for vasculogenesis and osteogenesis. First, we confirmed the differentiation capability of GM-PB CD34+ cells into osteoblasts in vitro. Second, local transplantation of GM-PB CD34+ cells on atelocollagen scaffold was performed in nude rats in a model of unhealing fractures. Immunostaining for human leukocyte antigen-ABC of tissue samples 1 week after fracture and cell therapy showed the superior incorporation after local transplantation compared with systemic infusion. Third, the effects of local transplantation of 10^5 (Hi), 10^4 (Mid), or 10^3 (Lo) doses of GM-PB CD34+ cells or phosphate-buffered saline (PBS) on fracture healing were compared. Extrinsic vasculogenic and osteogenic differentiation of GM-PB CD34+ cells, enhancement of the intrinsic angio-osteogenesis by recipient cells, augmentation of blood flow recovery at the fracture sites, and radiological and histological confirmation of fracture healing were observed only in the Hi and Mid groups but not in the Lo and PBS groups. These results strongly suggest that local transplantation of GM-PB CD34+ cells with atelocollagen scaffold is a feasible strategy for therapeutic vasculogenesis and osteogenesis needed for fracture healing. STEM CELLS *2008;26:1395–1405*

Disclosure of potential conflicts of interest is found at the end of this article.

INTRODUCTION

Adult stem/progenitor cells play important roles in tissue homeostasis and have important implications for regenerative medicine. A number of reports have suggested that stem cells derived from a variety of adult tissues are capable of maintaining, regenerating, and repairing other tissues derived from all three germ layers [1–3].

Endothelial progenitor cells (EPCs), which are involved in vascular development in the embryonic stage [4, 5], were first identified as CD34+ cells in adult peripheral blood (PB) [6]. Adult EPCs, originating mainly from bone marrow (BM), are mobilized into PB and recruited into neovascularization sites. Recruited EPCs contribute to postnatal neovascularization by proliferating, differentiating and migrating [6–8]. The therapeutic application of EPCs has been attempted for neovascularization in animal models of hind limb, myocardial, and cerebral ischemia/infarction [9–17] and wound healing [18].

Recent progress in stem cell biology has brought human EPCs/CD34+ cells to light for other fields of regenerative medicine. Eghbali-Fatourechi et al. [19] first identified circulating osteocalcin (OC)-positive cells in adult human, demonstrating osteogenic gene expression and mineralized nodule formation in vitro and bone regeneration in vivo. Chen et al. [20] identified osteoblast (OB) precursor cells in human BM CD34+ cells. Tondreau et al. [21] reported that granulocyte

Author contributions: Y.M.: conception and design, collection and/or assembly of data, data analysis and interpretation, manuscript writing; T.M. and A.K.: conception and design, administrative support, manuscript writing; R.K., T.S., H.I., S.-M.K., and M.M.: conception and design, administrative support; M.K. and T.A.: conception and design, financial support, final approval of manuscript.

Correspondence: Takayuki Asahara, M.D., Ph.D., Stem Cell Translational Research, Institute of Biomedical Research and Innovation/RIKEN Center for Developmental Biology, 2-2 Minatojima-Minamimachi, Chuo-ku, Kobe 650-0047, Japan. Telephone: 81-78-304-5772; Fax: 81-78-304-5263; e-mail: Asa777@aol.com; or Tomoyuki Matsumoto, M.D., Ph.D., Stem Cell Translational Research, Institute of Biomedical Research and Innovation/RIKEN Center for Developmental Biology, 2-2 Minatojima-Minamimachi, Chuo-ku, Kobe 650-0047, Japan. Telephone: 81-78-304-5772; Fax: 81-78-304-5263; e-mail: matsun@m4.dion.ne.jp Received October 18, 2007; accepted for publication March 23, 2008; first published online in STEM CELLS *EXPRESS* April 3, 2008. 1066-5099/2008/$30.00/0 doi: 10.1634/stemcells.2007-0820

colony-stimulating factor-mobilized peripheral blood (GM-PB) CD133+ cells, another EPC-enriched population, can act as mesenchymal stem cells and contribute to osteogenesis in vitro. These findings strongly suggest the therapeutic potential of BM-derived CD34+ cells for osteogenesis, as well as vasculogenesis. We previously reported that human circulating CD34+ cells, systemically transplanted into immunodeficient rats with nonhealing fracture, were recruited into fracture sites, contributed to a favorable environment for fracture healing by enhancing vasculogenesis and osteogenesis, and finally led to functional recovery from fracture [22]. Although our previous animal study demonstrating the efficacy of systemic transplantation of CD34+ cells may encourage the application of cell-based therapy in patients with unhealing fracture, local transplantation, but not systemic infusion, of CD34+ cells may need to be considered for future clinical trials for the following reasons: (a) intravenous infusion is generally known as a less safe method than local administration because of adverse systemic effects, and (b) local transplantation may allow reduction of effective cell dose compared with systemic administration, and this may overcome the critical issue in the clinical application: scarcity of circulating CD34+ cells in adults. Use of granulocyte colony-stimulating factor (G-CSF) is also a favorable method to harvest abundant CD34+ cells from adult PB in clinical situation.

In the current preclinical study, we proved the hypothesis that local transplantation of GM-PB CD34+ cells may contribute to fracture healing through vasculogenesis and osteogenesis at the lower dose compared with the systemic infusion used in our previous study [22]. We also demonstrated the in vitro differentiation potential of human GM-PB CD34+ cells into OBs as a supportive mechanistic study.

Materials and Methods

Preparation of Human Cells

We purchased human GM-PB CD34+ cells obtained from a healthy female (43 years old, African-American) and human BM total mononuclear cells (MNCs) obtained from a healthy female (25 years old, African-American) from Lonza (Valais, Switzerland, http://www.lonza.com/group/en.html).

Flow Cytometry Studies

Regular flow cytometric profiles were analyzed with a FACSCalibur analyzer (BD Biosciences, San Diego, http://www.bdbiosciences.com) and CELLQuest software (Becton, Dickinson and Company, Mountain View, CA, http://www.bd.com) as described previously [22].

Induction of Osteogenic Differentiation of GM-PB CD34+ Cells In Vitro

We seeded 5×10^4 BM-MNCs in six-well plates with α-minimum essential medium (α-MEM) (Gibco-BRL, Tokyo, http://www.gibcobrl.com) supplemented with 10% fetal bovine serum (FBS) (Vitromex, Vilshofen, Germany) and 2 mM L-glutamine (Gibco-BRL). After 2 weeks of culture, we collected the medium with floating cells and centrifuged it at 7,500*g* for 15 minutes at 4°C; we then collected the supernatant as conditioned medium (CM) and stored at −80°C for further use.

To induce mesenchymal stem cells from GM-PB CD34+ cells similarly to the previous method using BM-MNCs [21], we seeded 10^5 GM-PB CD34+ cells in six-well plates with α-MEM supplemented with 10% FBS, 2 mM L-glutamine, and 10% CM during the first 7 days of culture. Then, we cultured the cells in α-MEM supplemented with 10% FBS and 2 mM L-glutamine for the next 2 weeks.

Finally, to induce osteogenic differentiation, 10^5 cells were plated in six-well plates for 3 weeks under specific osteogenic conditions using α-MEM supplemented with 10% FBS, 2 mM L-glutamine, 60 μM ascorbic acid (Sigma-Aldrich, St. Louis, http://www.sigmaaldrich.com), 10 mM β-glycerophosphate (Sigma-Aldrich), and 0.1 μM dexamethasone (Sigma-Aldrich). Cells (10^5 cells) were also cultured with α-MEM supplemented with 10% FBS and 2 mM L-glutamine as a negative control.

Unhealing Fracture Model and Local/Systemic Transplantation of GM-PB CD34+ Cells

Female athymic nude rats (F344/N Jcl rnu/rnu; CLEA Japan, Tokyo, http://www.clea-japan.com) ages 8–12 weeks and weighing 150–170 g were used in this study. Nonhealing fracture was induced in femur with cauterizing periosteum according to the methods of Einhorn [23] and Kokubu et al. [24]. Immediately after the creation of nonhealing fracture, rats received local transplantation of 10^5 (Hi), 10^4 (Mid), or 10^3 (Lo) GM-PB CD34+ cells suspended in 100 μl of phosphate-buffered saline (PBS) using atelocollagen (Koken, Tokyo, http://www.kokenmpc.co.jp/english), which is a bovine-derived bioscaffold, or the same volume of PBS without cells using the same scaffold ($n = 15$ in the Hi group and $n = 12$ in all other groups). Atelocollagen was used as a bio-absorbable scaffold retaining the cells in the transplanted site [25, 26]. The left, unfractured femur of each animal served as a control. In addition, three rats received i.v. (systemic) transplantation of 10^5 GM-PB CD34+ cells suspended in 100 μl of PBS through the tail vein immediately after the creation of the fracture model.

Tissue Harvesting

Three rats receiving local or i.v. transplantation of 10^5 GM-PB CD34+ cells were sacrificed at week 1 for histological examination. Three rats in each group that received local transplantation were euthanized at weeks 2 and 4. Remaining rats receiving local transplantation were sacrificed at week 8. Bilateral femurs were harvested and quickly embedded as described previously [22].

Morphometric Evaluation of Capillary Density and OB Density

Histochemical staining with isolectin B4 (Vector Laboratories, Burlingame, CA, http://www.vectorlabs.com) as a rat endothelial cell (EC) marker or immunostaining for OC (Santa Cruz Biotechnology Inc., Santa Cruz, CA, http://www.scbt.com) as a rat and human OB marker was performed. Capillary or OB density was morphometrically evaluated as the average value in five randomly selected fields of soft tissue in the perifracture site. To address the location of chondrocytes in fractured sections, toluidine blue was used for counterstaining. All morphometric studies were performed by two blinded examiners.

Reverse Transcriptase Polymerase Chain Reaction Analysis of RNA Isolated from GM-PB CD34+ Cells and Tissue Samples at the Perifracture Site

Total RNA was obtained from GM-PB CD34+ cells and the rat tissues in perifracture sites at week 2 using Trizol (Life Technologies, Gaithersburg, MD, http://www.lifetech.com) according to the manufacturer's instructions. The synthesization of first-strand cDNA and polymerase chain reaction (PCR) were performed as described previously [22]. Subsequently, PCR products were visualized in 1.5% ethidium bromide-stained agarose gels. Human umbilical vein endothelial cells and human OBs (NHOst cells; Cambrex) were used for positive controls for human-specific endothelial and bone-related genes.

To avoid interspecies cross-reactivity of the primer pairs between human and rat genes, we designed human-specific primers using Oligo software (Takara Bio, Shiga, Japan, http://www.takara-bio.com). Each primer sequence is shown in supplemental online Information 1. No primers showed cross-reactivity to rat genes (data not shown).

Real-Time PCR Analysis to Detect Expression of Cytokines in Recipients Following Human GM-PB CD34+ Cell Transplantation

Total RNA was obtained from the rat tissues at perifracture sites at week 2 as described for reverse transcription (RT)-PCR analysis. After the first-strand cDNA was synthesized, the converted cDNA samples (2 μl) were amplified in triplicate by real-time PCR (ABI Prism 7700, Applied Biosystems, Foster City, CA, http://www3.appliedbiosystems.com/index.htm) in a final volume of 20 μl using SYBR Green Master Mix reagent (Applied Biosystems). Melting curve analysis was performed to ensure that only a single product was amplified using Dissociation Curves software (Applied Biosystems). Specificity of the reactions was confirmed by 2.0% agarose gel electrophoresis. Results were obtained using sequence detection software (ABI Prism 7700) and evaluated using Excel (Microsoft, Redmond, WA, http://www.microsoft.com). Each primer sequence is shown in supplemental online Information 2.

Physiological Assessment of Tissue Perfusion by Laser Doppler Perfusion Imaging

Laser Doppler perfusion imaging (LDPI) (Moor Instruments, Wilmington, DE, http://www.moor.co.uk) [27, 28] was used to measure blood flow in both legs at 0, 1, 2, and 3 weeks postfracture. The ratio of fractured to intact (contralateral) blood flow was calculated to evaluate serial blood flow recovery after fracture.

Immunohistochemical Staining

To detect the transplanted human cells in the rat tissue, immunohistochemistry was performed with following human-specific antibodies: human leukocyte antigen (HLA)-ABC (BD Pharmingen, San Diego, http://www.bdbiosciences.com/index_us.shtml) to detect various lineage of human cells, *Ulex europaeus* lectin type 1 (UEA-1) (Vector Laboratories) for human ECs, human-specific osteocalcin (hOC) (Biomedical Technologies, Inc., Stoughton, MA, http://www.btiinc.com/index.html) for human OBs, and smooth muscle actin (SMA) for both human and rat smooth muscle cells. The secondary antibodies for each immunostaining were as follows: Alexa Fluor 594-conjugated goat anti-mouse IgG_1 (Molecular Probes, Tokyo, http://probes.invitrogen.com) for HLA-ABC staining, Cy3-conjugated streptavidin (Jackson Immunoresearch Laboratories, West Grove, PA, http://www.jacksonimmuno.com) for UEA-1 staining, Alexa Fluor 488-conjugated goat anti-mouse IgG_{2a} (Molecular Probes) for SMA, and Cy3-conjugated AffiniPure goat anti-rabbit IgG(H+L) (Jackson Immunoresearch Laboratories) for hOC. 4,6-Diamidino-2-phenylindole solution was applied for 5 minutes for nuclear staining.

Radiographic Assessment of the Fracture Healing

Radiographs of the fractured hind limbs were taken on weeks 0, 2, 4, and 8 following creation of the fracture. Fracture union was identified by the presence of a bridging callus on two cortices. Radiographs of each animal were examined by three blinded observers.

Histological Assessment of the Fracture Healing

Toluidine blue staining was performed to histologically evaluate the process of endochondral ossification at weeks 2, 4, and 8. The degree of fracture healing was evaluated using a five-point scale proposed by Allen et al. [29].

Statistical Analysis

The results were statistically analyzed using a software package (Statview 5.0; Abacus Concepts Inc, Berkeley, CA, http://www.abacus.com/abacus/home). All values were expressed as mean ± SE. Paired *t* tests were performed for comparison of data before and after treatment, and unpaired *t* tests were performed for comparison of local and i.v. transplantation. The multiple comparisons among groups were made using a one-way analysis of variance. Post hoc analysis was performed by Fisher's Protected Least Significant Difference test. The comparison of radiological results was performed with a χ^2 test. A probability value of $<.05$ was considered to denote statistical significance.

RESULTS

Phenotypic Characterization of GM-PB CD34+ Cells

GM-PB CD34+ cells from the healthy females used in this study were analyzed by flow cytometry. GM-PB CD34+ cell fraction was mainly positive for CD133, CD31, c-Kit, and CD45 but negative for kinase insert domain protein receptor and CD14 (supplemental online Fig. 1A). RT-PCR analysis of the GM-PB CD34+ cells revealed weak expression of the human-specific gene of CD31 (hCD31) and OC (hOC) but no expression of VE-cadherin (hVE-cad) and collagen1A1 (hCol1A1) (supplemental online Fig. 1B). RT-PCR analysis of the bovine-derived atelocollagen that we used as a scaffold showed no expression of human-specific genes, suggesting no cross-reaction of human-specific primers with bovine mRNAs.

In Vitro Differentiation of Human GM-PB CD34+ Cells into OBs

During the primary culture for mesenchymal stem cell induction, part of the GM-PB CD34+ cells exhibited a fibroblast-like spindle shape (Fig. 1A), proliferating quickly to form colonies (Fig. 1B). Treatment for 3 weeks with specific conditions for osteogenic induction resulted in a morphological transformation of the cells from long and spindle-like into a cuboidal shape (Fig. 1C). In contrast, no transformation was observed in the negative control group (Fig. 1D). As shown in Figure 1E, following osteogenic induction, matrix mineralization (calcium deposition) was clearly demonstrated by alizarin red staining. In contrast, no mineralization was observed in negative control wells (Fig. 1F). As shown in Figure 1G, mRNA of hOC and hCol1A1 was highly expressed in the CD34+ cells after osteogenic induction compared with those not induced. These results indicate that human GM-PB CD34+ cells are capable of differentiating into OBs under specific culture conditions.

More Efficient Incorporation of Human GM-PB CD34+ Cells at Fracture Site Following Local Transplantation Compared with Systemic Infusion

To test the potential therapeutic superiority of local transplantation over systemic infusion, rats received 10^5 GM-PB CD34+ cells locally or intravenously and were sacrificed 1 week later to obtain tissue samples at the fracture sites. Immunostaining for HLA-ABC was performed to quantify the number of recruited human cells in the rat granulation area (Fig. 2A, 2B) and newly bone formed area (Fig. 2D, 2E). The double immunostaining for HLA-ABC and SMA demonstrated more abundant recruitment of human cells in the granulation area compared with the inner layer of SMA-positive smooth muscle cells, which were morphologically compatible with endothelial cells in arterioles, in both groups (Fig. 2A, 2B). The number of human cells in the granulation area was significantly higher in the local transplantation group compared with the i.v. infusion group (local, 105.6 ± 14.8; i.v., 38.0 ± 16.6 cells per mm^2; $p < .05$) (Fig. 2C). Similarly, the number of human cells in the newly formed bone area was significantly higher in the local transplantation group than in the i.v. infusion group (local, 96.0 ± 10.5; i.v., 37.9 ± 15.4 cells per mm^2; $p < .05$) (Fig. 2F). These findings strongly indicate that local transplantation is superior to i.v. infusion in terms of efficiency of human GM-PB CD34+ cell incorporation into fracture sites.

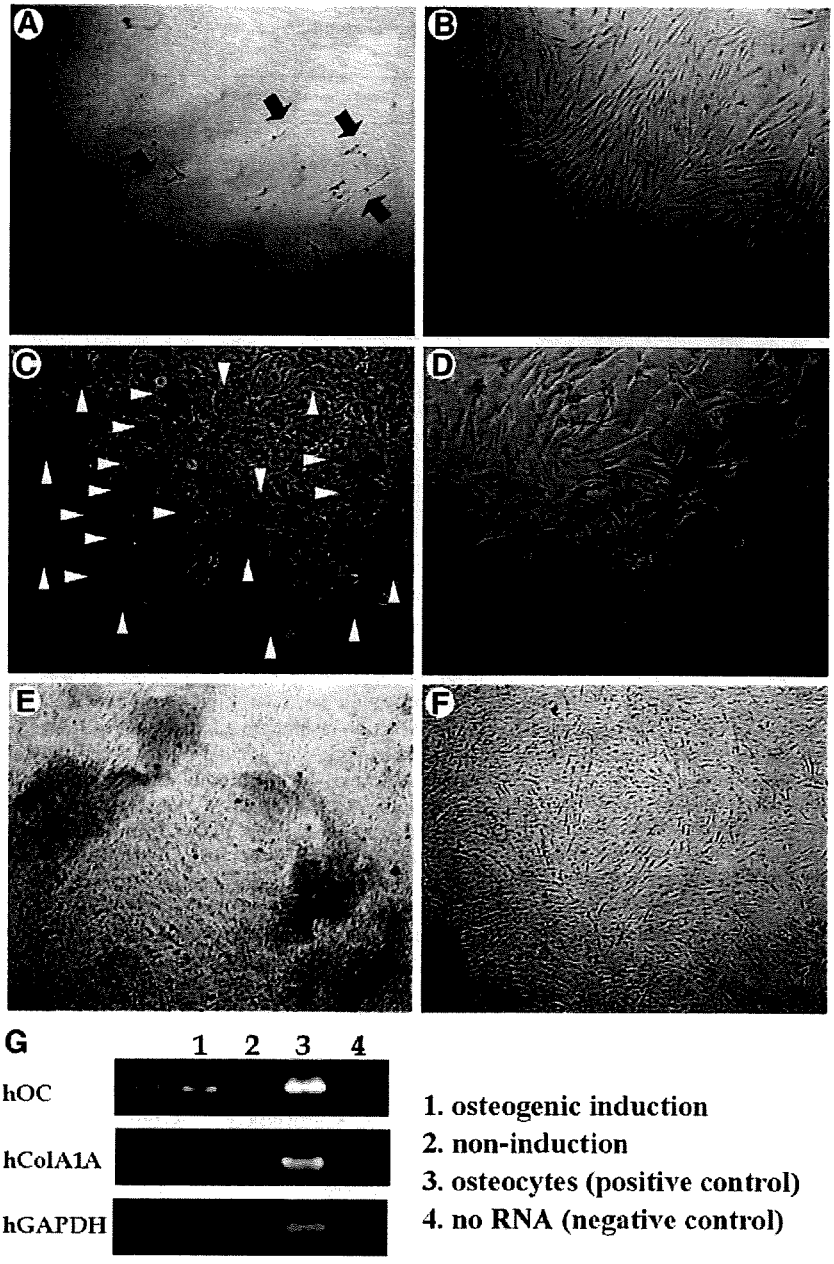

Figure 1. Osteogenic differentiation of granulocyte colony-stimulating factor-mobilized peripheral blood (GM-PB) CD34+ cells in vitro. **(A, B):** Morphology of the GM-PB CD34+ cells, which were cultured in α-minimal essential medium (α-MEM) supplemented with 10% fetal bovine serum (FBS), 2 mM L-glutamine, and 10% conditioned medium (CM) during the first 7 days and in the same medium without CM for the next 1 week, changed into fibroblast-like spindle shape (×200) **(A)**. Then, these spindle-shaped cells proliferated quickly to form colonies (×40) **(B)**. **(C, D):** After osteogenic induction with α-MEM supplemented with 10% FBS, 2 mM L-glutamine, 60 μM ascorbic acid, 10 mM β-glycerophosphate, and 0.1 μM dexamethasone, the cell morphology changed from spindle-shaped to a cuboidal shape (arrowheads) (×40) **(C)**. In contrast, no transformation was observed in cultured CD34+ cells with α-MEM supplemented with 10% FBS and 2 mM L-glutamine only (no osteogenic induction) (×40) **(D)**. **(E, F):** In wells with osteogenesis-inducing conditions, the matrix mineralization was clearly demonstrated by alizarin red staining, indicating existence of calcium **(E)**. In contrast, no mineralization was observed in noninducing conditions (×40) **(F)**. **(G):** The mRNA of hOC and hCol1A1 was markedly expressed in osteogenesis-induced cells but not in noninduced cells. Abbreviations: hGAPDH, human glyceraldehyde-3-phosphate dehydrogenase; hOC, human-specific osteocalcin.

Vasculogenesis and Osteogenesis Induced by Human GM-PB CD34+ Cells

Next, we performed experiments to characterize the transplanted human CD34+ cells incorporating into fracture sites. To histologically validate the phenomenon of human cell-derived vasculogenesis, histochemical staining for UEA-1, a human-specific EC marker, was performed using the tissue samples obtained 2 weeks after local cell transplantation. Differentiated human ECs in the vasculature of the perifracture area were detected as UEA-1-positive cells in the Hi and Mid GM-PB CD34+ cell groups but not in the Lo and PBS groups (Fig. 3A–3F). These findings suggest that GM-PB CD34+ cells have the potential to differentiate into ECs; however, transplantation of more than 10^4 CD34+ cells may be necessary for significant vasculogenesis. To further verify this phenomenon, RT-PCR analysis of tissue RNA isolated from the perifracture site for human-specific EC markers (hVE-cad and hCD31) was performed (Fig. 3G). The expression ratio of hVE-cad to rat glyceraldehyde-3-phosphate dehydrogenase (rGAPDH) was significantly greater in the Hi group than in all others; the ratio was also higher in the Mid group than in the Lo and PBS groups (Hi, 0.579 ± 0.043; Mid, 0.399 ± 0.023; Lo, 0.197 ± 0.011; PBS, 0.191 ± 0.018; $p < .01$ for Hi vs. Lo or PBS group; $p < .05$ for Hi vs. Mid and for Mid vs. Lo or PBS group). The expression ratio of hCD31 to rGAPDH was also greater in the Hi group than in the other groups, and the ratio was higher in the Mid group than in the Lo and PBS groups. The ratio was also significantly higher in the Lo group than in the PBS group (Hi, 0.974 ± 0.064; Mid, 0.563 ± 0.023; Lo, 0.429 ± 0.025; PBS group, 0.159 ± 0.011; $p < .01$ for Hi vs. PBS group; $p < .05$ for Hi vs. Mid or Lo, for Mid vs. Lo or PBS, and for Lo vs. PBS group) (Fig. 3H).

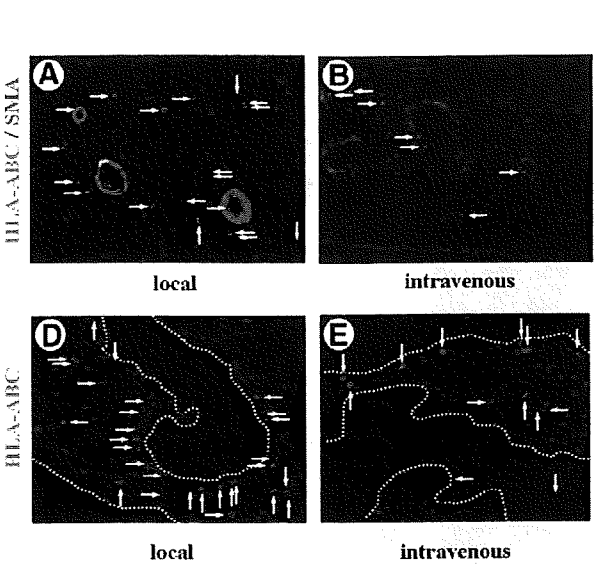

Figure 2. Recruitment efficiency of locally or intravenously transplanted human CD34+ cells. Number of human CD34+ cells incorporating into the fracture site 1 week after the cell transplantation was compared between local and i.v. administration groups. **(A, B):** Representative double immunostaining for HLA-ABC (red) and SMA (green) in granulation areas of local **(A)** and i.v. **(B)** transplantation groups. **(C):** Number of HLA-ABC-positive cells in granulation area. *, $p < .05$ ($n = 3$ in each group). **(D, E):** Representative immunostaining for HLA-ABC in newly formed bone area in local **(D)** and i.v. **(E)** transplantation groups. **(F):** Number of HLA-ABC-positive cells in newly formed bone area. *, $p < .05$ ($n = 3$ in each group). Abbreviations: HLA, human leukocyte antigen; SMA, smooth muscle actin.

To identify osteogenesis from human CD34+ cells, immunohistochemical staining for human-specific OC, an OB marker, was performed using tissue samples obtained 2 weeks after cell transplantation. Differentiated human OBs derived from high and middle doses of GM-PB CD34+ cells were detected as hOC-positive cells in the perifracture area (Fig. 3I, 3J), whereas hOC-positive cells were not identified in the low-dose group of GM-PB CD34+ cells or the PBS group (Fig. 3K, 3L). These findings suggest that transplanted GM-PB CD34+ cells may have the potential to differentiate into OBs; however, a greater than middle dose of CD34+ cells may be necessary for significant osteogenesis, as suggested in the vasculogenesis assessment. RT-PCR analysis also demonstrated dose-dependent expression of human-specific bone-related markers (hOC and hCol1A1) following human GM-PB CD34+ cell transplantation (Fig. 3M). The expression ratio of hOC to rGAPDH was significantly greater in the Hi group than in the other groups (Hi, 0.591 ± 0.032; Mid, 0.279 ± 0.021; Lo, 0.287 ± 0.014; PBS, 0.288 ± 0.011; $p < .05$ for Hi vs. Mid, Lo, or PBS group). The expression ratio of hCol1A1 to rGAPDH was also significantly greater in the Hi group than in the other groups, as well as in the Mid group compared with the Lo and PBS groups (Hi, 0.988 ± 0.077; Mid, 0.366 ± 0.030; Lo, 0.227 ± 0.021; PBS, 0.031 ± 0.004, respectively; $p < .01$ for Hi vs. PBS group; $p < .05$ for Hi vs. Mid or Lo, for Mid vs. Lo or PBS, and for Lo vs. PBS groups) (Fig. 3N).

These results indicate that human GM-PB CD34+ cells dose-dependently differentiate into both EC and OB lineages in the fracture-induced environment. For efficient vasculogenesis and osteogenesis, local transplantation of at least 10^4 CD34+ cells may be essential in this animal model.

Enhancement of Intrinsic Angiogenesis and Osteogenesis in Animals Receiving GM-PB CD34+ Cells

Enhanced angiogenesis and osteogenesis by the paracrine effect of the transplanted cells on recipients' cells were confirmed by immunostaining for rat-specific markers. Vascular staining with isolectin B4, a rat-specific marker for EC, using tissue samples collected 2 weeks postfracture, demonstrated enhancement of intrinsic neovascularization around the endochondral ossification area in animals treated with high and middle doses of GM-PB CD34+ cells (Fig. 4A). Capillary density was significantly greater in the Hi group compared with the other groups, as well as in the Mid group compared with the Lo and PBS groups (Hi, 1,136.8 ± 95.5; Mid, 928.7 ± 61.6; Lo, 752.5 ± 49.3; PBS, 616.5 ± 57.4 cells per mm^2, respectively; $p < .01$ for Hi vs. PBS group; $p < .05$ for Hi vs. Mid or Lo group and for Mid vs. Lo or PBS group) (Fig. 4B).

OB staining with anti-rat OC using tissue samples collected 2 weeks postfracture revealed augmentation of intrinsic osteogenesis in the area of new bone formation in animals treated with high and middle doses of GM-PB CD34+ cells (Fig. 4C). OB density was significantly greater in the Hi group than in the other groups, and density in the Mid group was significantly higher than that in the PBS group (Hi, 641.3 ± 54.3; Mid, 399.6 ± 21.3; Lo, 301.7 ± 12.4; PBS group, 213.6 ± 19.2 cells per mm^2, respectively; $p < .01$ for Hi vs. PBS group; $p < .05$ for Hi vs. Mid or Lo group and for Mid vs. PBS group) (Fig. 4D).

A possible explanation for the enhancement of intrinsic angiogenesis and osteogenesis following CD34+ cell therapy is the upregulation of angiogenesis- and osteogenesis-related cytokines at the perifracture site. Accordingly, we performed real-time RT-PCR to quantify the expression of rat vascular endothelial growth factor (rVEGF) and rat bone morphogenetic protein 2 (rBMP-2) around the fracture sites. The expression ratio of rVEGF to rGAPDH at week 2 was greater in animals receiving a high dose of GM-PB CD34+ cells compared with other groups, and the ratio in the middle-dose group was higher than that in the low-dose and PBS groups (Hi, 1.131 ± 0.284; Mid, 1.085 ± 0.269; Lo, 1.037 ± 0.215; PBS, 1.035 ± 0.231, respectively; $p < .01$ for Hi vs. Lo or PBS group; $p < .05$ for Hi vs. Mid group and for Mid vs. Lo or PBS group) (Fig. 4E). The expression ratio of rBMP-2 to rGAPDH at week 2 was also significantly greater in animals receiving a high dose of GM-PB CD34+ cells compared with other groups, and the ratio in the middle-dose group was higher than that in the low-dose and PBS groups (Hi, 1.028 ± 0.276; Mid, 0.991 ± 0.271; Lo, 0.923 ± 0.216; PBS, 0.907 ± 0.244, respectively; $p < .01$ for Hi vs. Lo or PBS and for Mid vs. PBS group; $p < .05$ for Hi vs. Mid group and for Mid vs. Lo group) (Fig. 4F). These results indicate that high and middle doses of human GM-PB CD34+ cells enhance both intrinsic angiogenesis and osteogenesis, at least in part by upregulating rVEGF and rBMP-2 at the fracture sites.

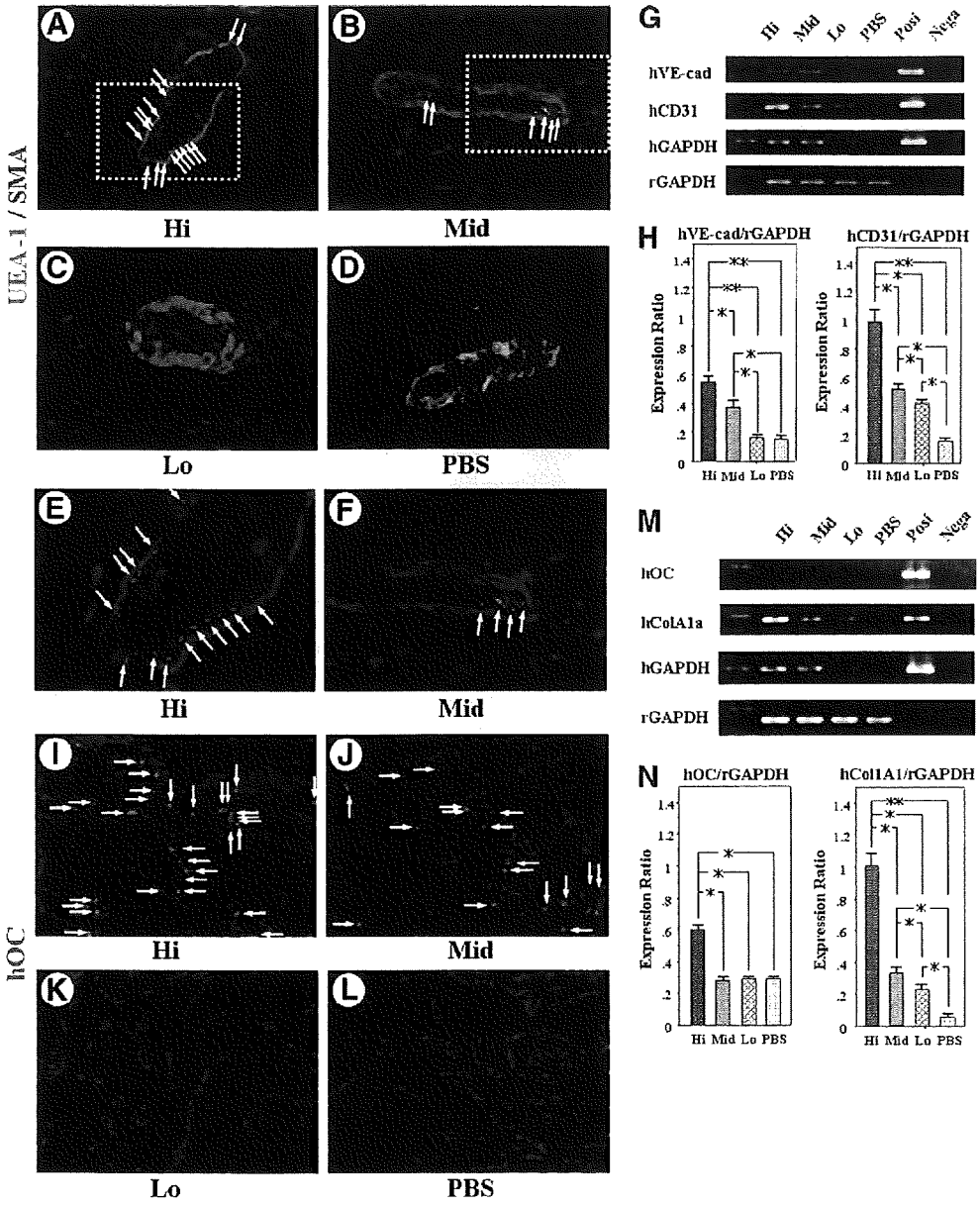

Figure 3. Fracture site vasculogenesis and osteogenesis derived from human CD34+ cells. **(A–F):** Representative double immunostaining for UEA-1 (red) and SMA (green) using tissue samples of the fracture sites at week 2 (original magnification, ×200 **[A–D]**, ×400 **[E, F]**). Differentiated human endothelial cells (ECs) identified as UEA-1 positive cells (red) were observed only in animals receiving a high dose (Hi) **(A, E)** or a middle dose (Mid) **(B, F)** of CD34+ cells but not in those treated with a low dose (Lo) **(C)** or PBS **(D)**. **(G):** Reverse transcriptase (RT) PCR analysis of tissue RNA isolated from the perifracture sites demonstrated the expression of human-specific EC markers (hVE-cad, hCD31) in animals treated with Hi, Mid, and Lo doses of CD34+ cells but not in animals receiving PBS. Cultured human umbilical vein endothelial cells were used for the Posi. For the Nega, no RNA was applied. **(H):** The ratio of gene expression of hVE-cad to rGAPDH in perifracture site was significantly greater in the Hi group than in other groups, as well as in the Mid group compared with the Lo and PBS groups. The ratio of gene expression of hCD31 to rGAPDH was significantly greater in the Hi group than in the other groups, as well as in the Mid group compared with Lo and PBS groups. **, $p < .01$; *, $p < .05$ ($n = 4$ in each group). **(I–L):** Representative immunostaining for hOC (green) using samples collected from fracture sites at week 2 (×100). Differentiated human osteoblasts (OBs) identified as hOC-positive cells (green) were observed in animals receiving Hi **(I)** and Mid **(J)** doses, but not in the Lo **(K)** and PBS **(L)** groups. **(M):** RT-PCR analysis using RNA isolated from the perifracture sites demonstrated the expression of human-specific bone-related markers (hOC and hCol1A1) in animals treated with Hi, Mid, and Lo doses of CD34+ cells but not in animals receiving PBS. Cultured human OBs were used for the Posi. **(N):** The ratio of gene expression of hOC to rGAPDH in perifracture sites was significantly greater in the Hi group than in the other groups, and the ratio of gene expression of hCol1A1 to rGAPDH was significantly greater in the Hi group than in the other groups, as well as in the Mid group compared with the Lo and PBS groups. **, $p < .01$; *, $p < .05$ ($n = 4$ in each group). Abbreviations: hGAPDH, human glyceraldehyde-3-phosphate dehydrogenase; Hi, 10^5; hOC, human-specific osteocalcin; hVE-cad, human VE-cadherin; Lo, 10^3; Mid, 10^4; Nega, negative control; PBS, phosphate-buffered saline; Posi, positive control; rGAPDH, rat glyceraldehyde-3-phosphate dehydrogenase; SMA, smooth muscle actin; UEA-1, *Ulex europaeus* lectin type 1.